

Chemical Vapor Deposition of Ruthenium-based Layers by the Single-Source Approach

Janine Jeschke,^a Stefan Möckel,^a Marcus Korb,^a Tobias Rüffer,^a Khaybar Assim,^a Marcel Melzer,^{b,c} Gordon Herwig,^d Colin Georgi,^{b,c} Stefan E. Schulz,^{b,c} and Heinrich Lang^{a,*}

*a) Technische Universität Chemnitz, Faculty of Natural Sciences, Institute of Chemistry,
Inorganic Chemistry, 09107 Chemnitz, Germany.*

*b) Fraunhofer Institute for Electronic Nano Systems (ENAS), Technologie-Campus 3, 09126
Chemnitz, Germany.*

*c) Technische Universität Chemnitz, Center for Microtechnologies, 09107 Chemnitz,
Germany.*

*d) Technische Universität Chemnitz, Faculty of Natural Sciences, Institute of Physics,
Chemical Physics, 09107 Chemnitz, Germany.*

Supporting Information

Contents

Crystallographic Data	3
Selected Bond Lengths and Angles	4
TG Studies	5
SEM Images of Layers A–G	6
EDX Spectra	9
XPS Data	10
Applied parameters for the peak deconvolution in XPS analyses	10
XPS detail spectra.....	10
XRPD	14
^1H and $^{13}\text{C}\{^1\text{H}\}$ NMR Spectra of Ruthenium Complexes 4a–g	15

Crystallographic Data

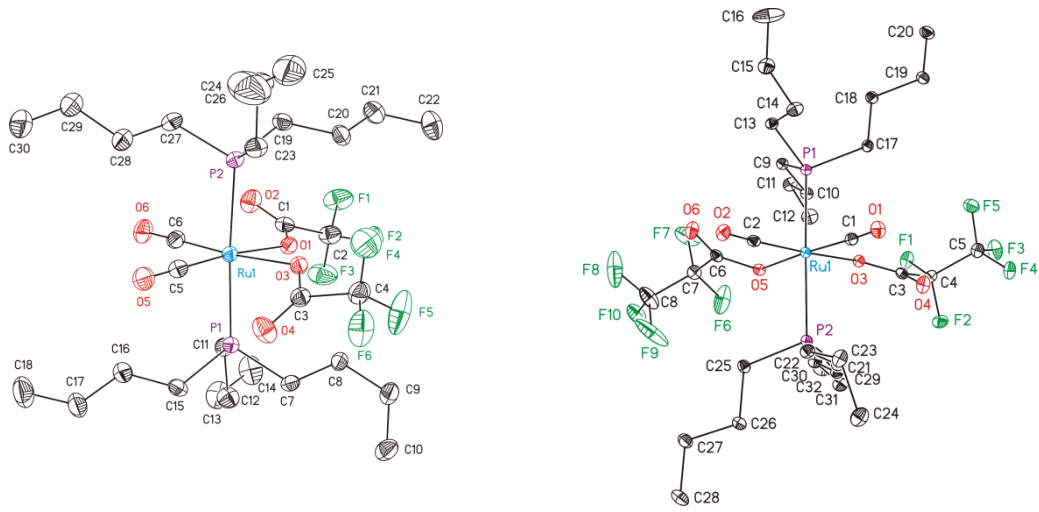


Figure S1. ORTEP diagram (30 % probability level) of the molecular structures of **4f** (left) and **4g** (right) with the atom numbering scheme. All hydrogen and disordered atoms have been omitted for clarity.

Selected Bond Lengths and Angles

Table S2. Selected bond distances (\AA) and angles ($^\circ$) for complexes **4b,c** and **4e–g**.

	4b	4c	4e	4f	4g
Ru–O	2.1018(14)	2.1010(13)	2.100(2)	2.1046(17)	2.1099(15)
		2.1037(12)		2.0937(17)	2.1074(15)
Ru–C	1.873(2)	1.866(2)	1.892(3)	1.866(3)	1.877(2)
		1.873(2)		1.862(3)	1.869(2)
Ru–P	2.3906(5)	2.3856(5)	2.3844(8)	2.4063(7)	2.4102(6)
		2.3910(5)		2.4096(7)	2.3993(6)
C≡O	1.143(3)	1.144(2)	1.134(4)	1.140(3)	1.143(3)
		1.141(2)		1.141(3)	1.144(3)
C–O	1.230(3)	1.230(2)	1.221(4)	1.268(3)	1.224(3)
	1.291(3)	1.280(2)	1.294(4)	1.214(3)	1.267(3)
		1.231(2)		1.204(3)	1.220(3)
		1.290(2)		1.274(3)	1.269(3)
P–Ru–P	173.03(3)	173.041(18)	173.04(4)	176.23(3)	171.11(2)
P–Ru–C	92.93(7)	92.70(6)	92.44(9)	91.68(9)	93.57(7)
	92.05(7)	92.90(6)	92.60(9)	91.27(9)	93.86(7)
		92.87(6)		91.07(9)	92.58(7)
		91.48(6)		91.31(9)	92.82(7)
P–Ru–O	84.58(4)	90.20(4)	85.20(6)	91.99(5)	89.16(4)
	90.17(4)	84.70(4)	89.44(6)	84.46(5)	84.00(4)
		85.23(4)		85.23(5)	83.95(4)
		89.57(4)		92.55(5)	89.66(4)
C–Ru–C	88.83(13)	87.65(8)	87.13(19)	89.94(13)	87.34(9)
O–Ru–O	82.27(8)	83.55(5)	79.27(11)	80.24(7)	83.75(6)
C–Ru–O	175.90(7)	176.19(7)	175.53(10)	174.50(10)	176.28(8)
	94.50(8)	94.44(7)	96.84(12)	94.40(10)	94.64(8)
		176.70(7)		173.25(10)	177.09(8)
		94.51(7)		95.67(10)	94.40(8)
Ru–C–O	175.11(19)	173.12(18)	174.8(3)	178.0(3)	175.0(2)
		174.12(17)		177.2(3)	174.9(2)

TG Studies

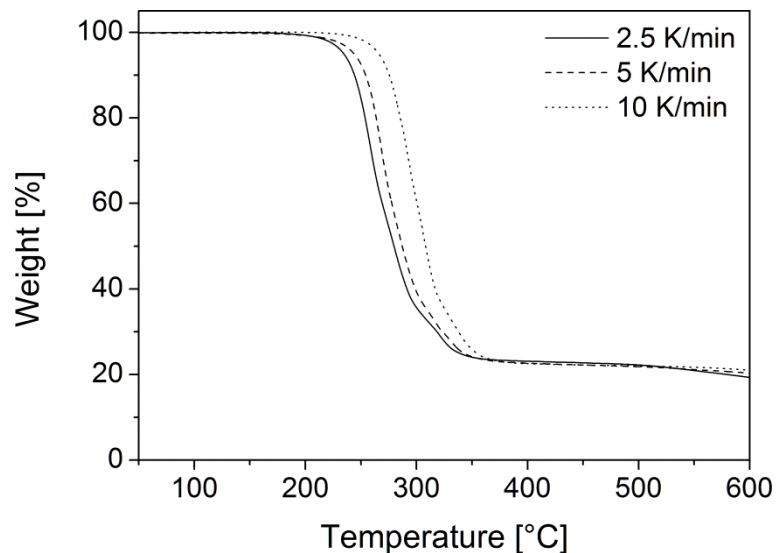
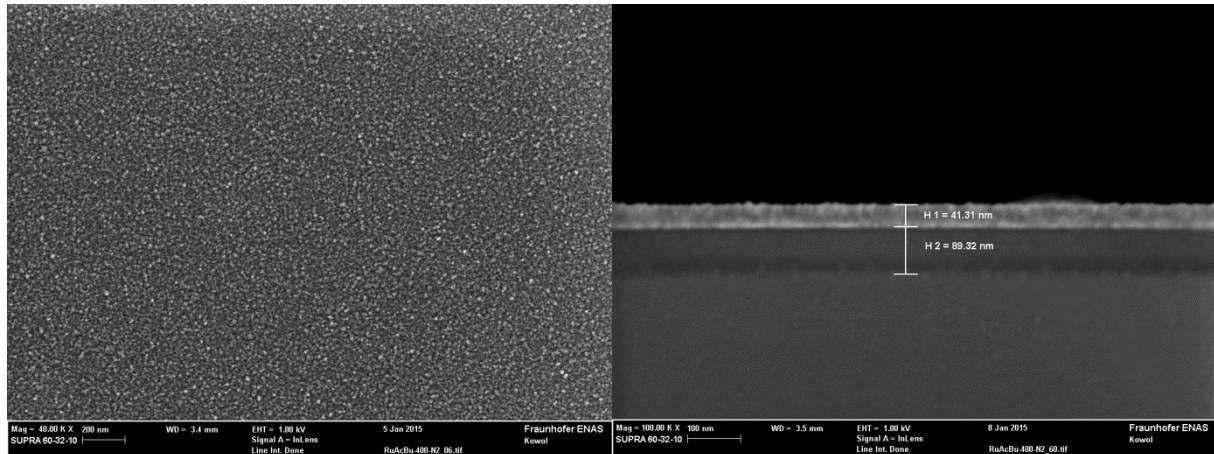


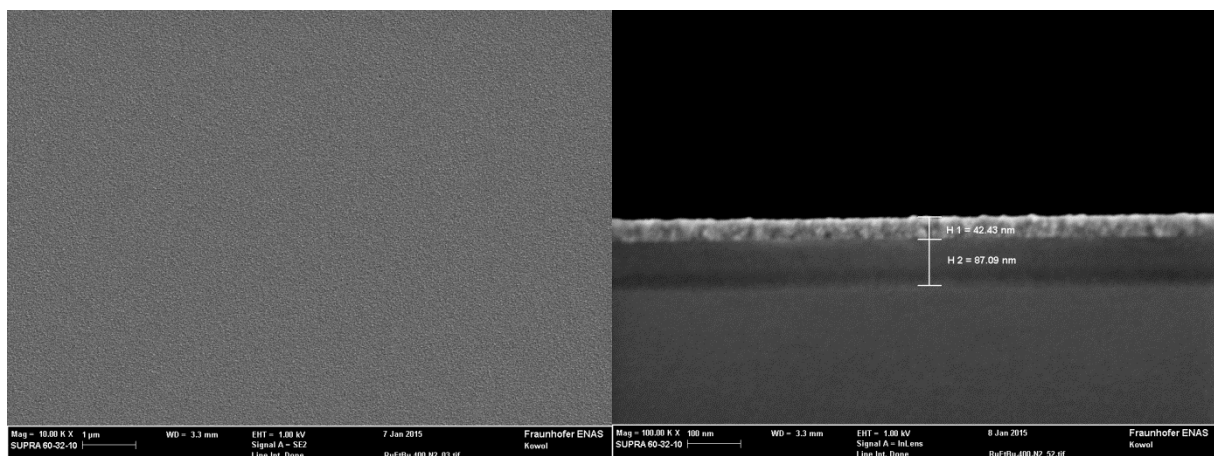
Figure S3. TG traces of **4e** at varying heating rates; gas flow N_2 $60 \text{ mL}\cdot\text{min}^{-1}$.

SEM Images

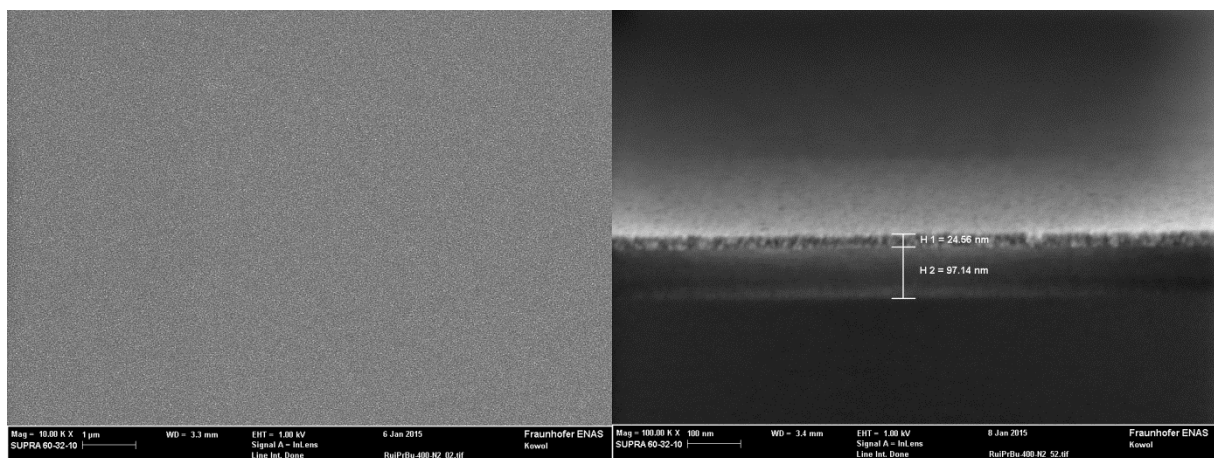
Layer A



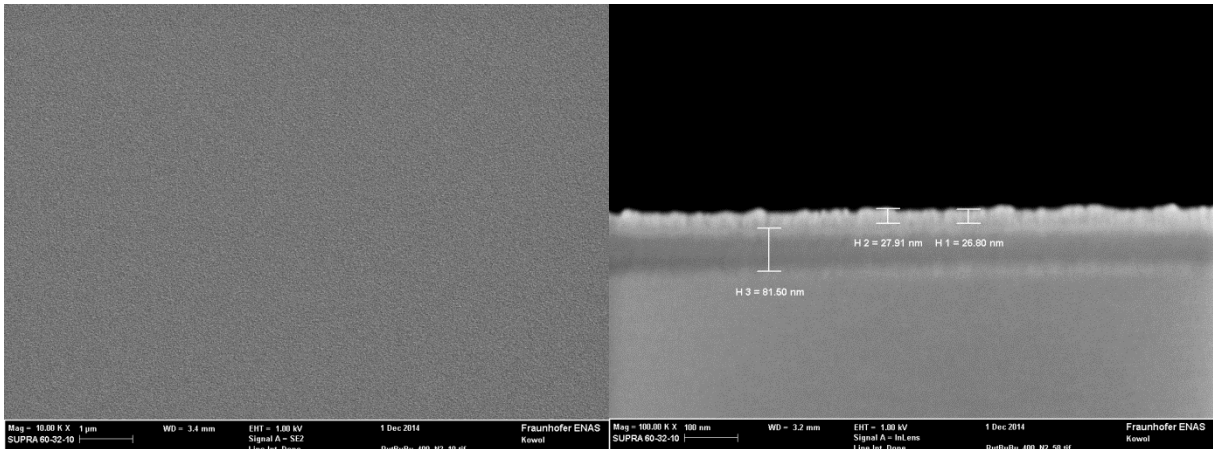
Layer B



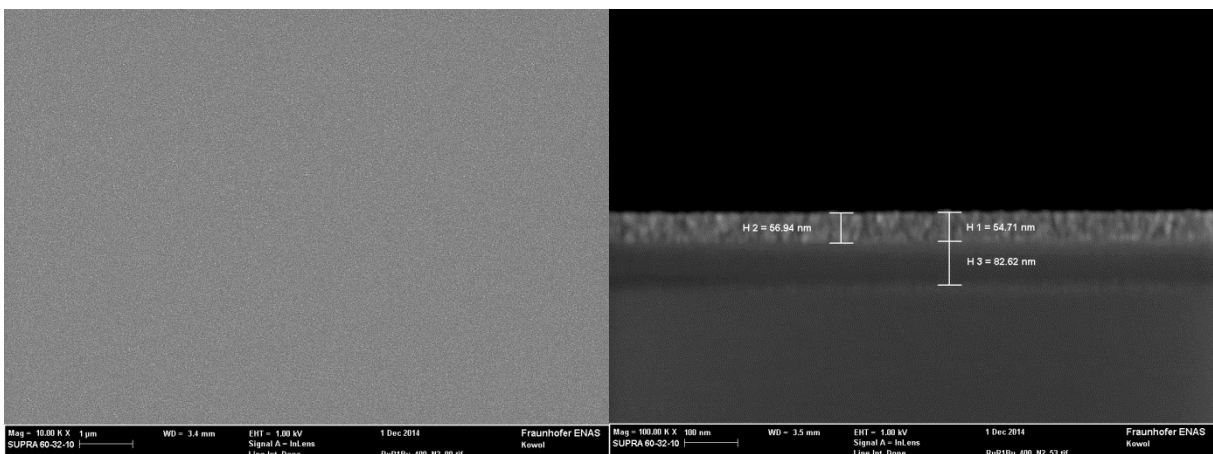
Layer C



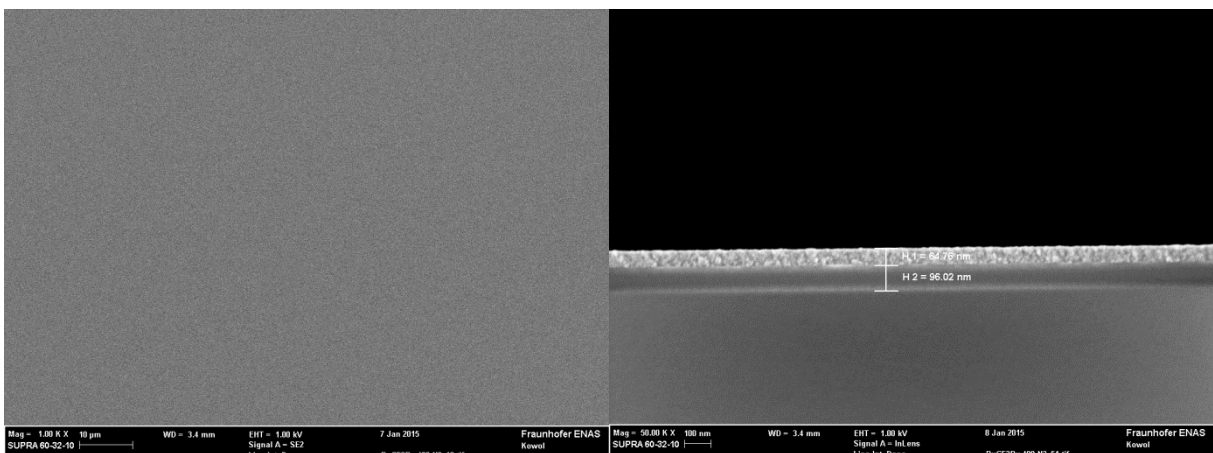
Layer D



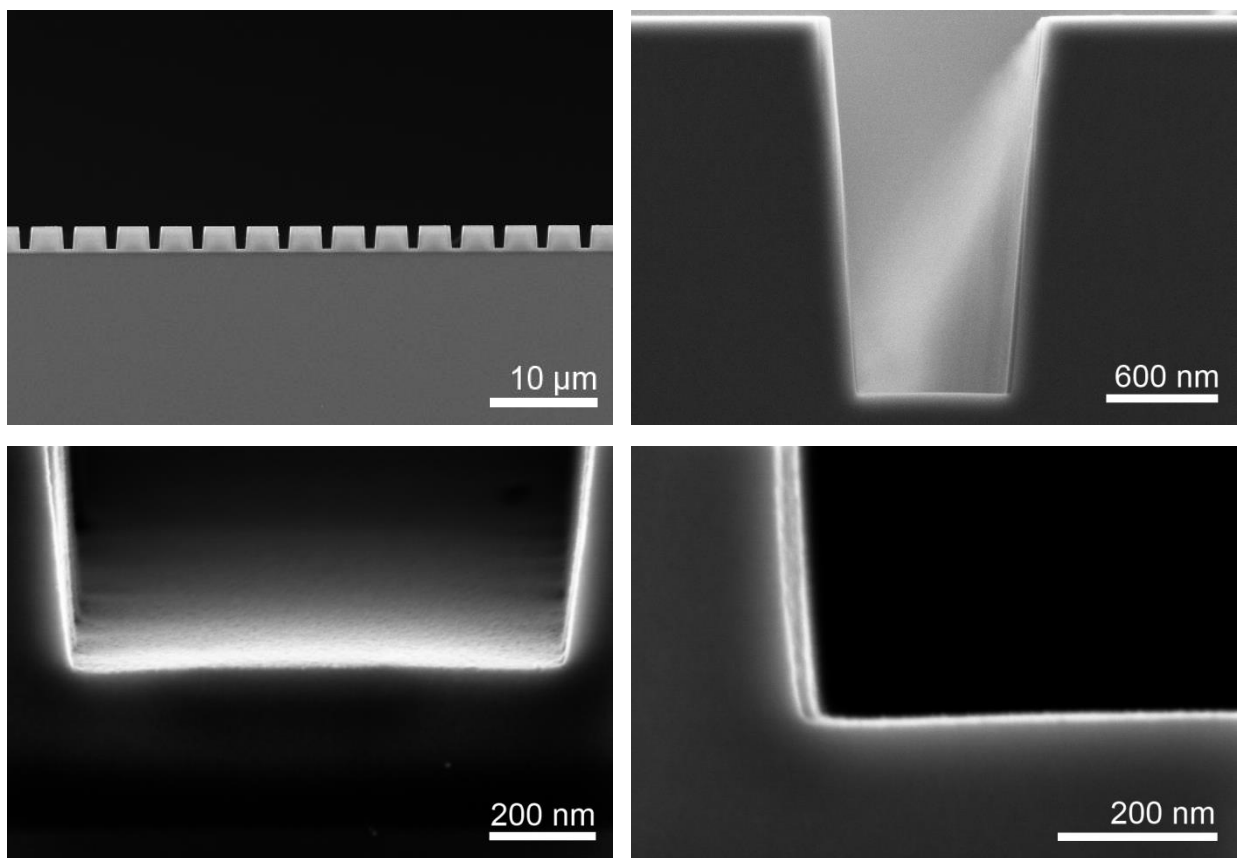
Layer E



Layer F



Layer H



EDX Spectra

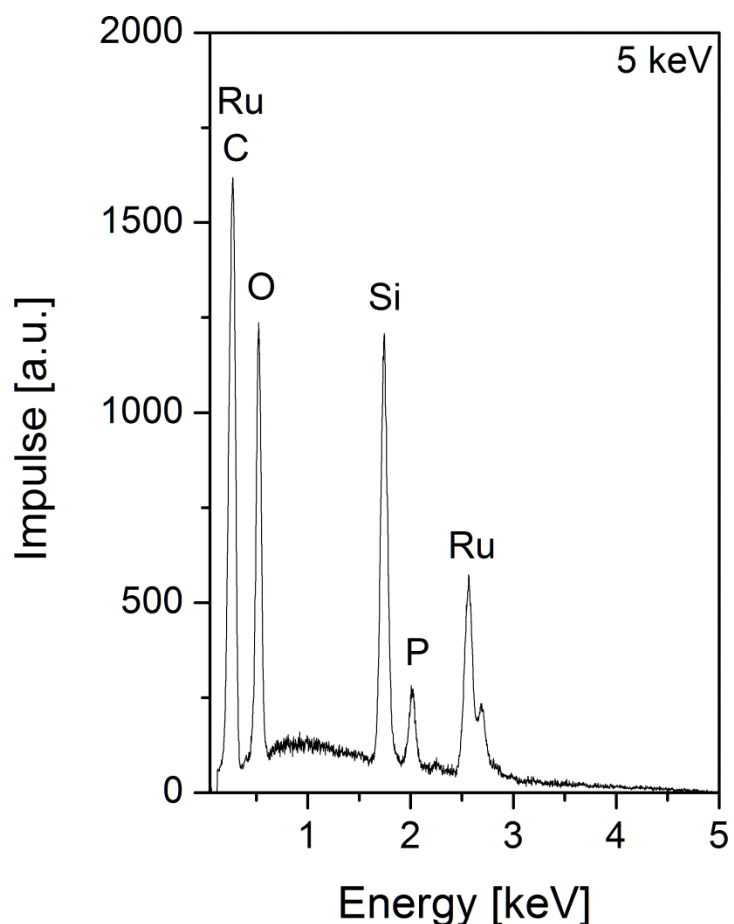


Figure S4. Representative EDX spectra obtained from layer E (Table 2) showing the characteristic pattern of ruthenium and the presence of phosphorus, silicon, oxygen and carbon.

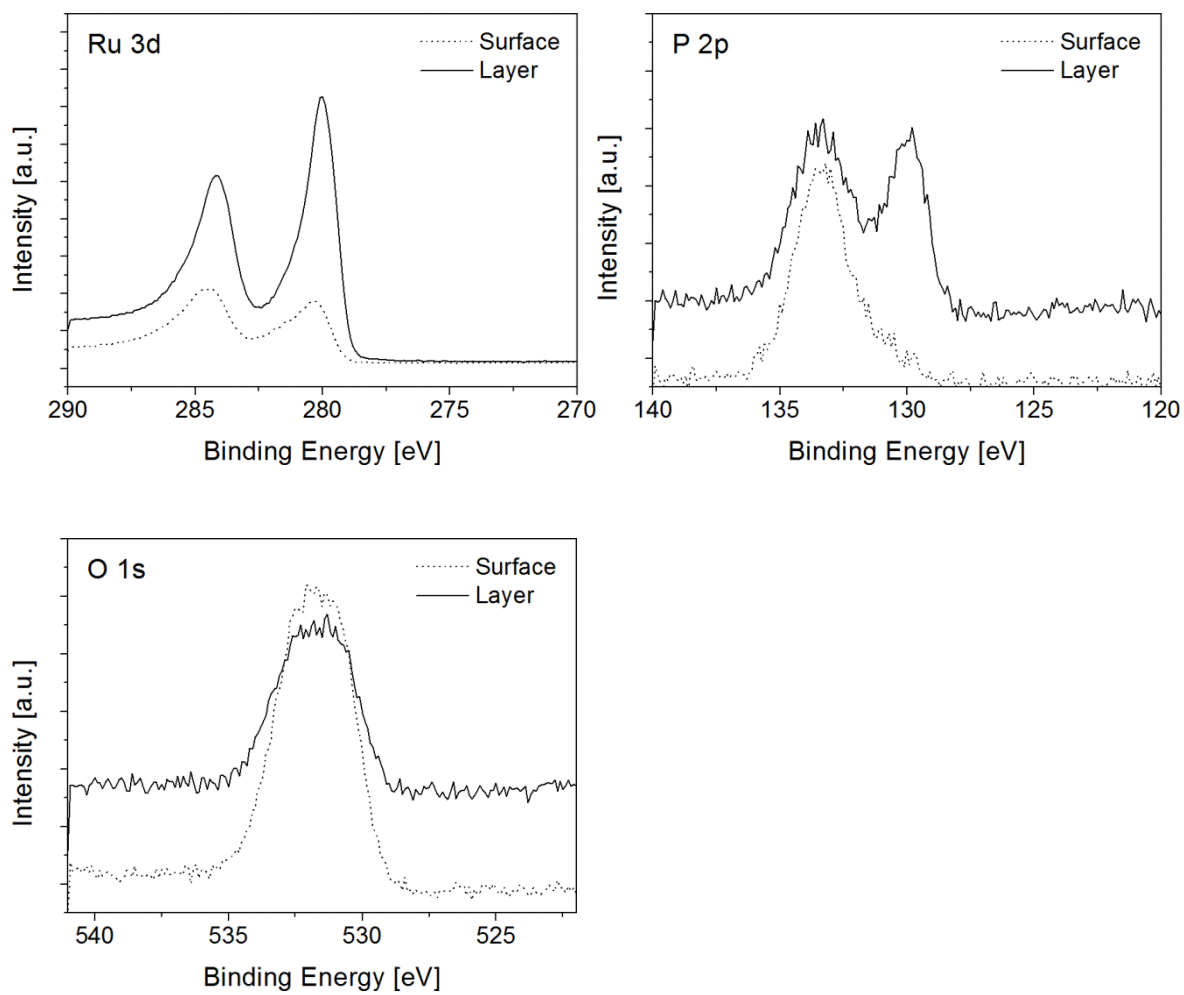
XPS Data

Table S5. Applied parameters for the peak deconvolution in XPS analyses.

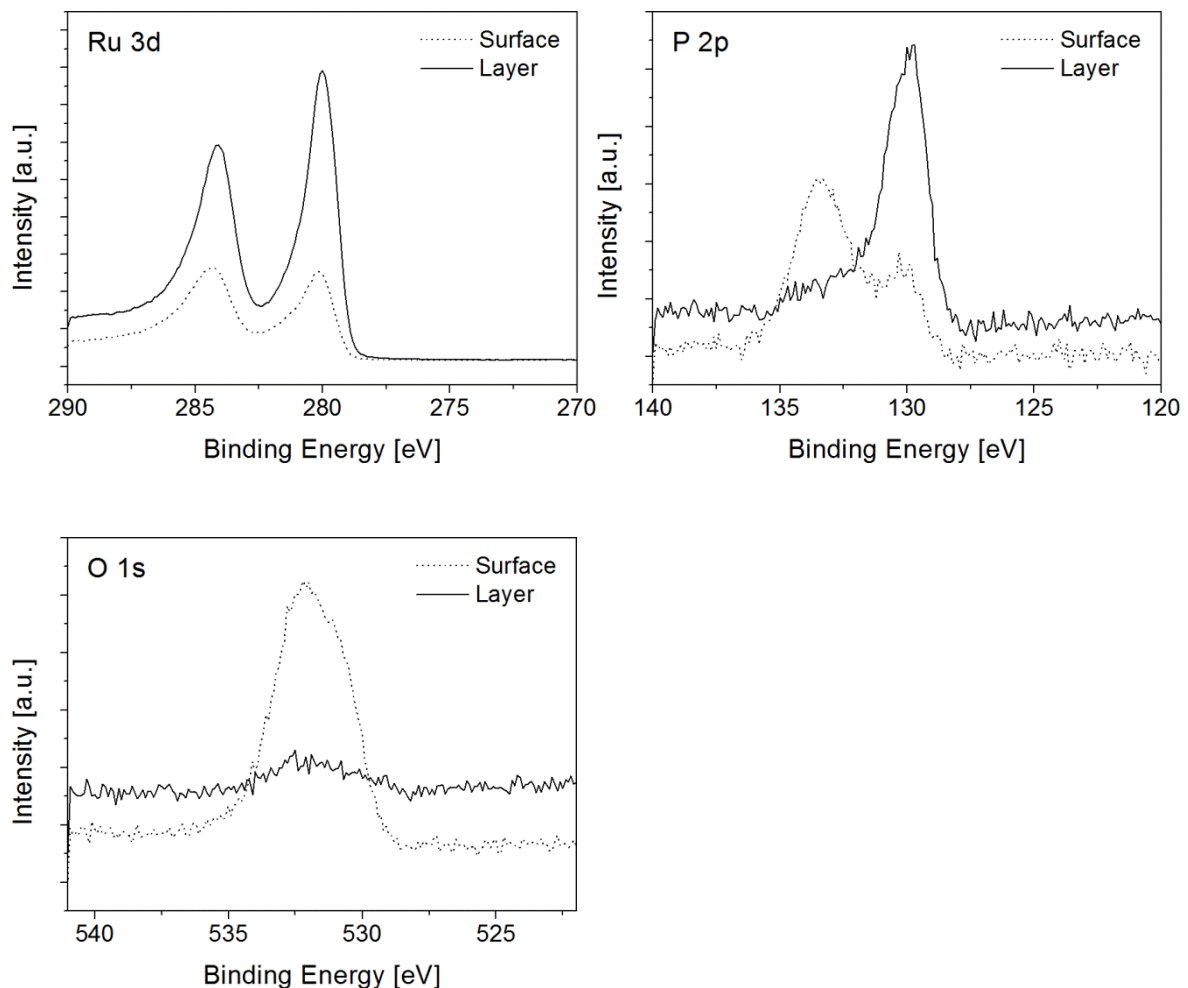
Peak	Ru 3d 5/2	Ru 3d 3/2	RuO ₂ 3d 5/2	RuO ₂ 3d 3/2	C 1s
Line shape	Gaussian-Lorentzian, GL(25) + exponential tail				GL(25)
Pos. [eV]	280.5-279.5	Ru 3d 5/2 + 4.2	282.0-280.6	RuO ₂ 3d 5/2 + 4.2	285.5 – 284.5

XPS detail spectra

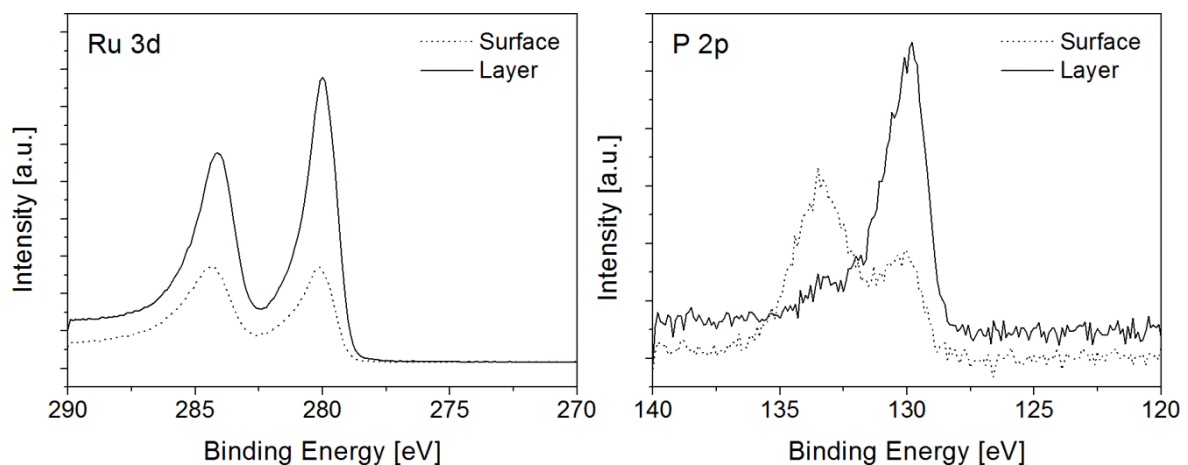
Layer A

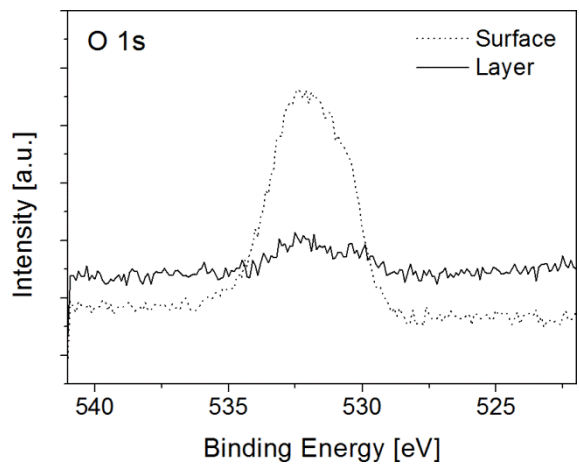


Layer B

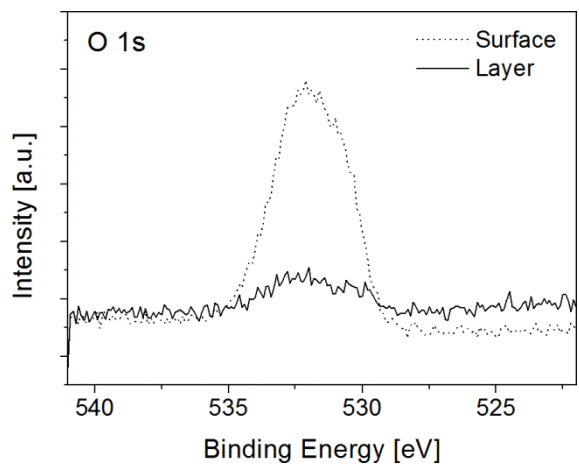
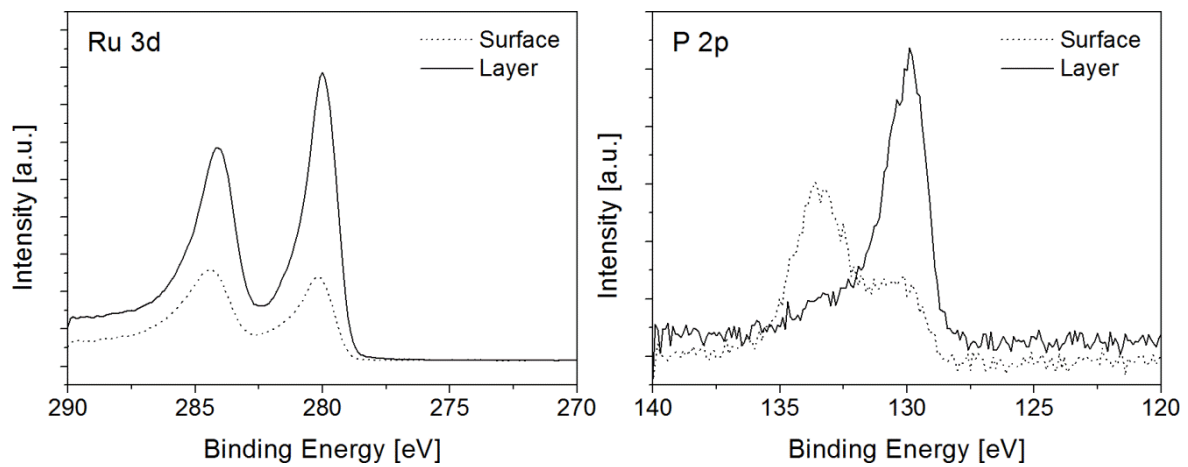


Layer C

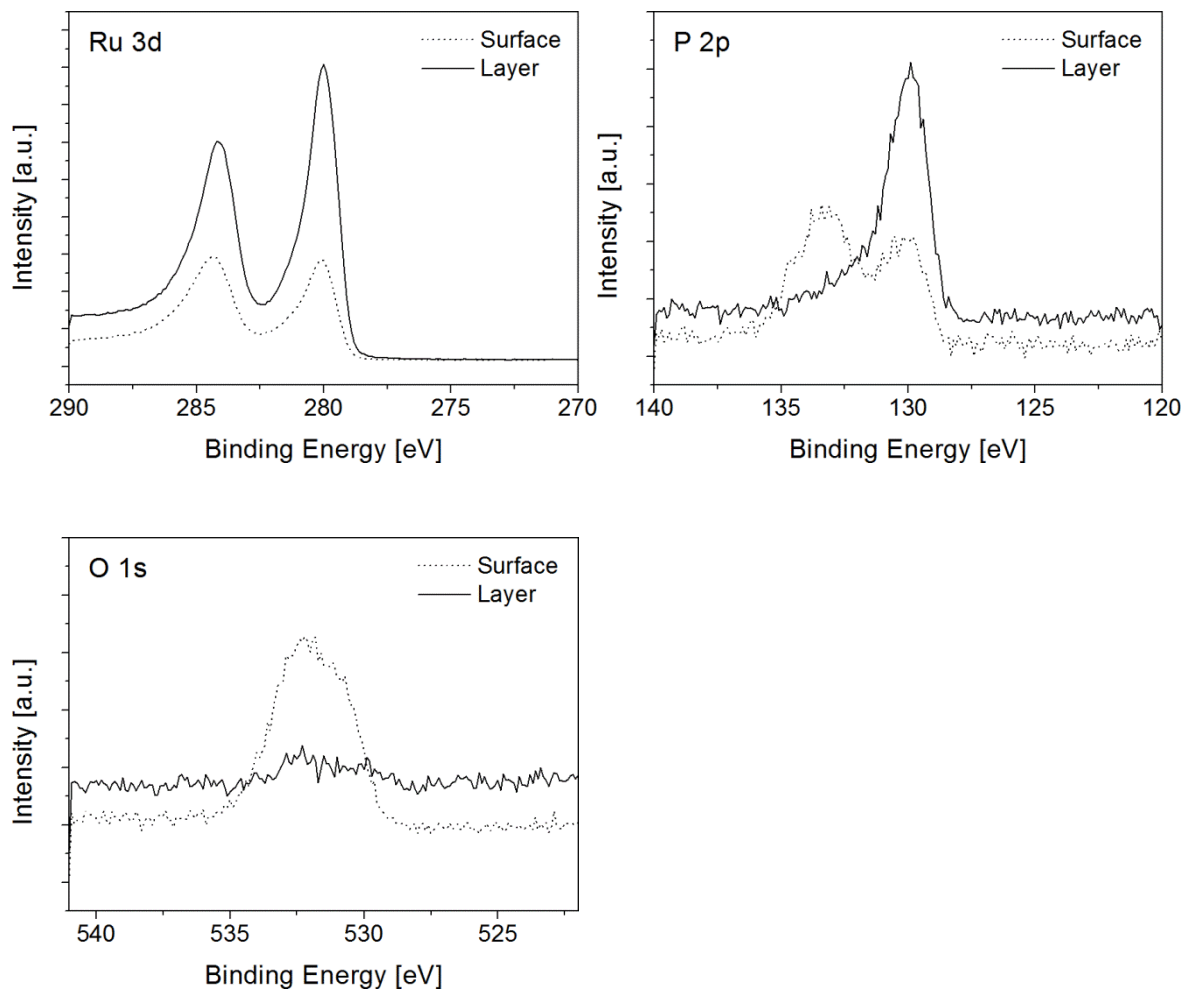




Layer D



Layer F



XRPD

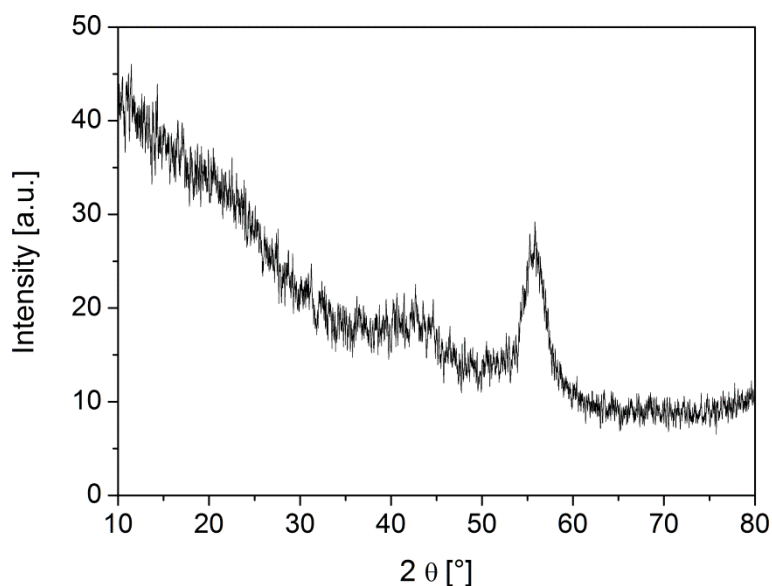
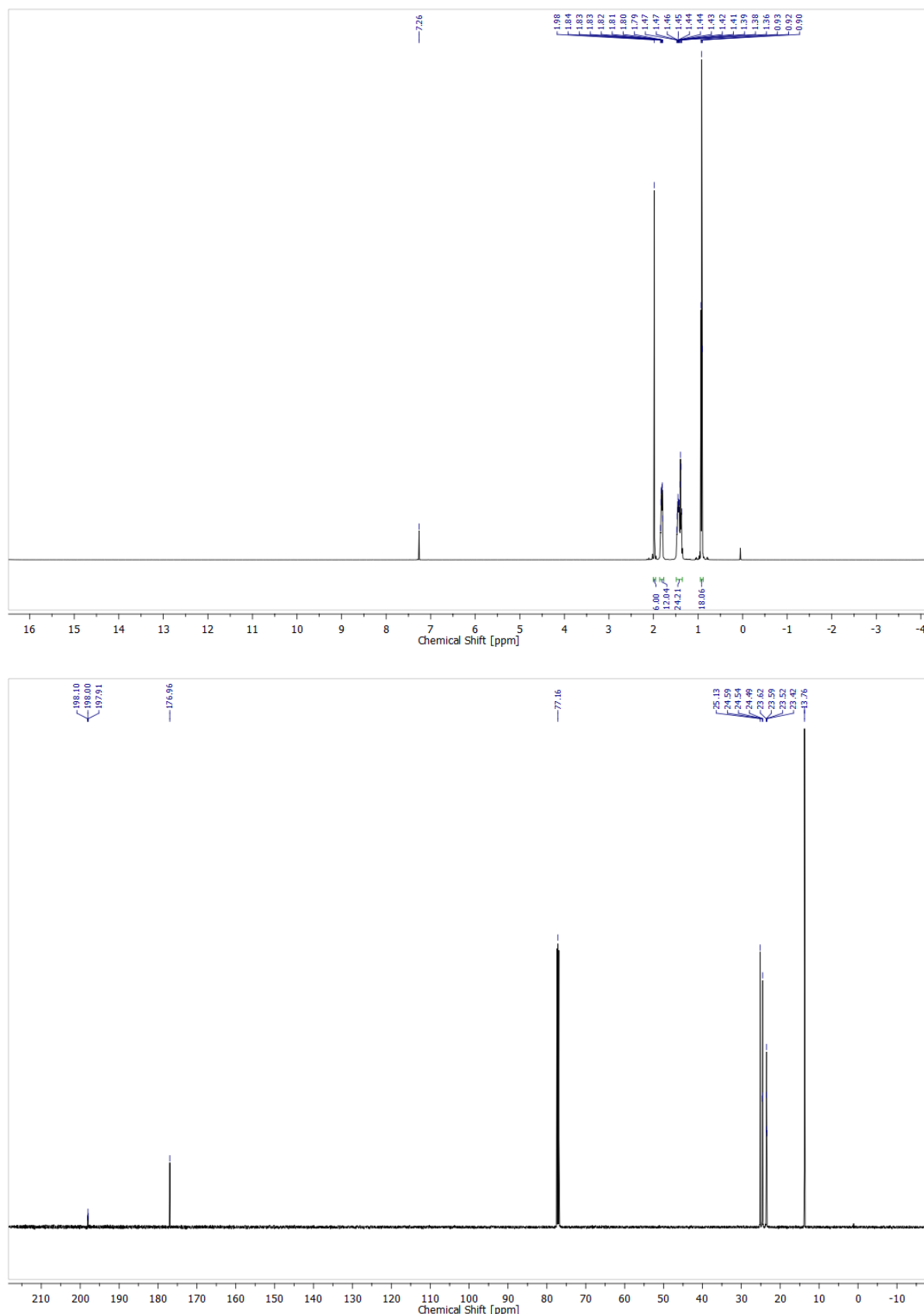


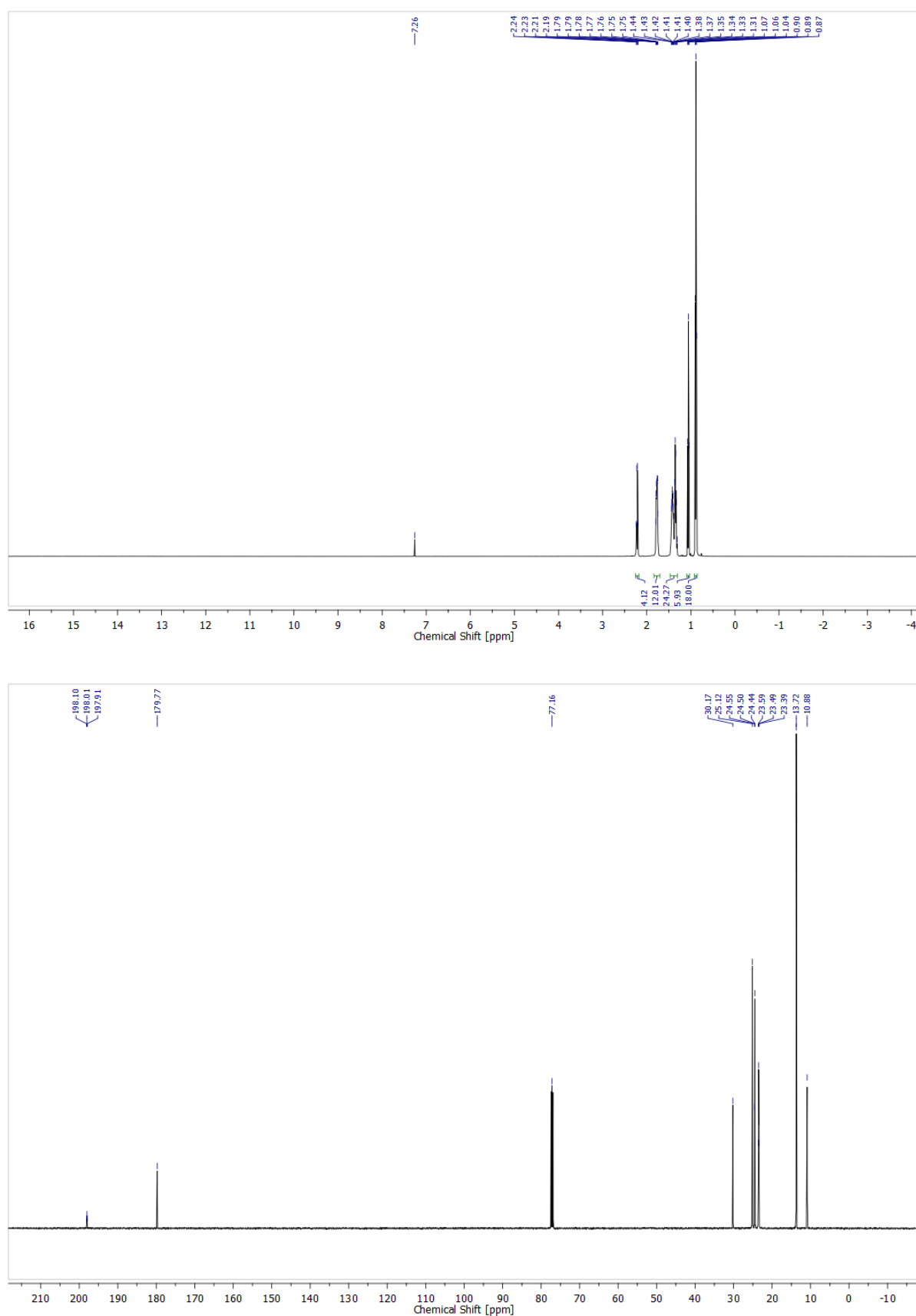
Figure S6. Representative diffractogram of layer E (Table 2) measured under grazing incidence. The diffractogram was recorded using Cu-K_{α1} radiation ($\lambda = 1.5405 \text{ \AA}$) with a Ge(111) monochromator.

^1H and $^{13}\text{C}\{^1\text{H}\}$ NMR Spectra of Ruthenium Complexes 4a–g in CDCl_3

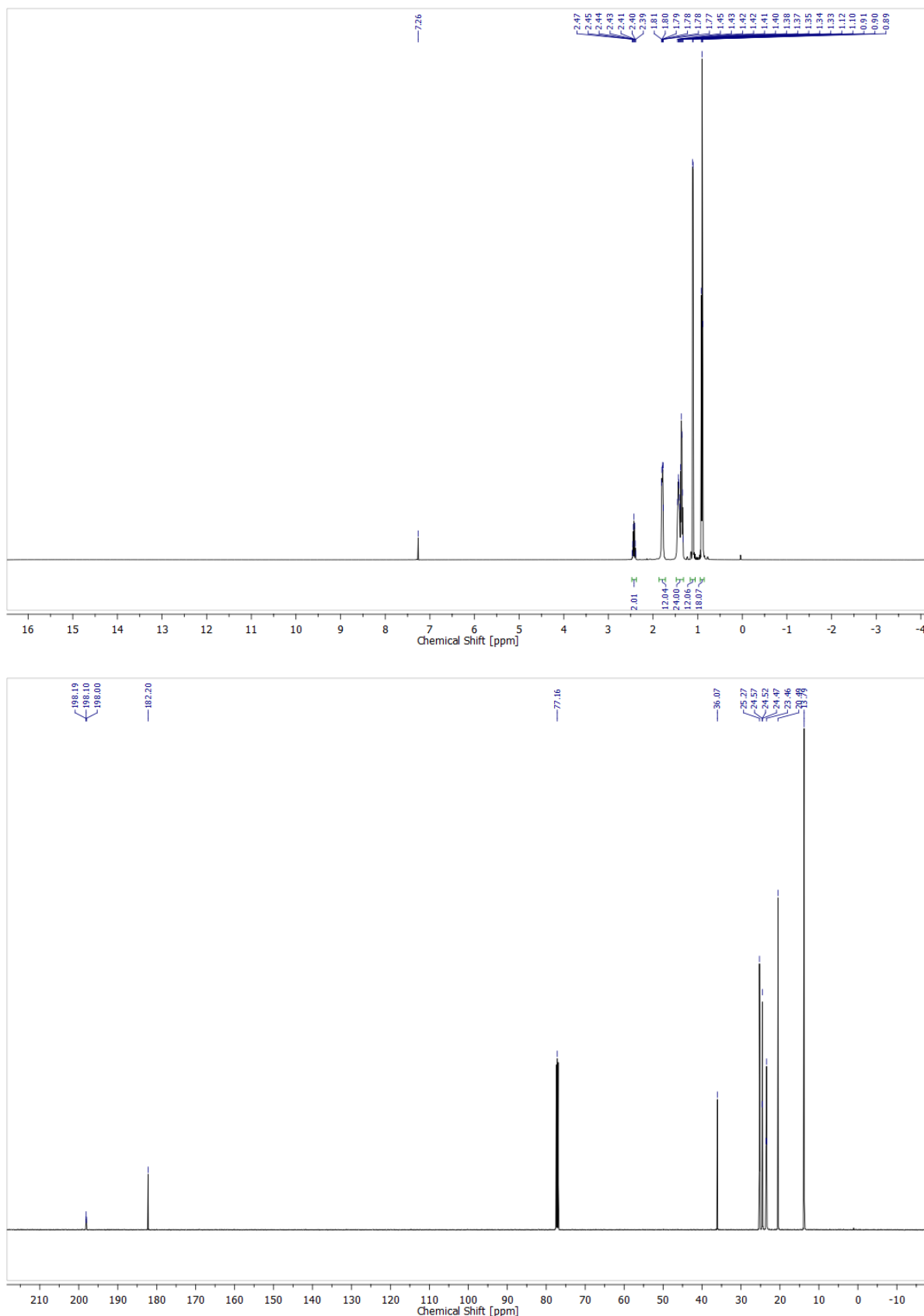
$\text{Ru}(\text{CO})_2(\text{P}^n\text{Bu}_3)_2(\text{O}_2\text{CCH}_3)_2$ (**4a**)



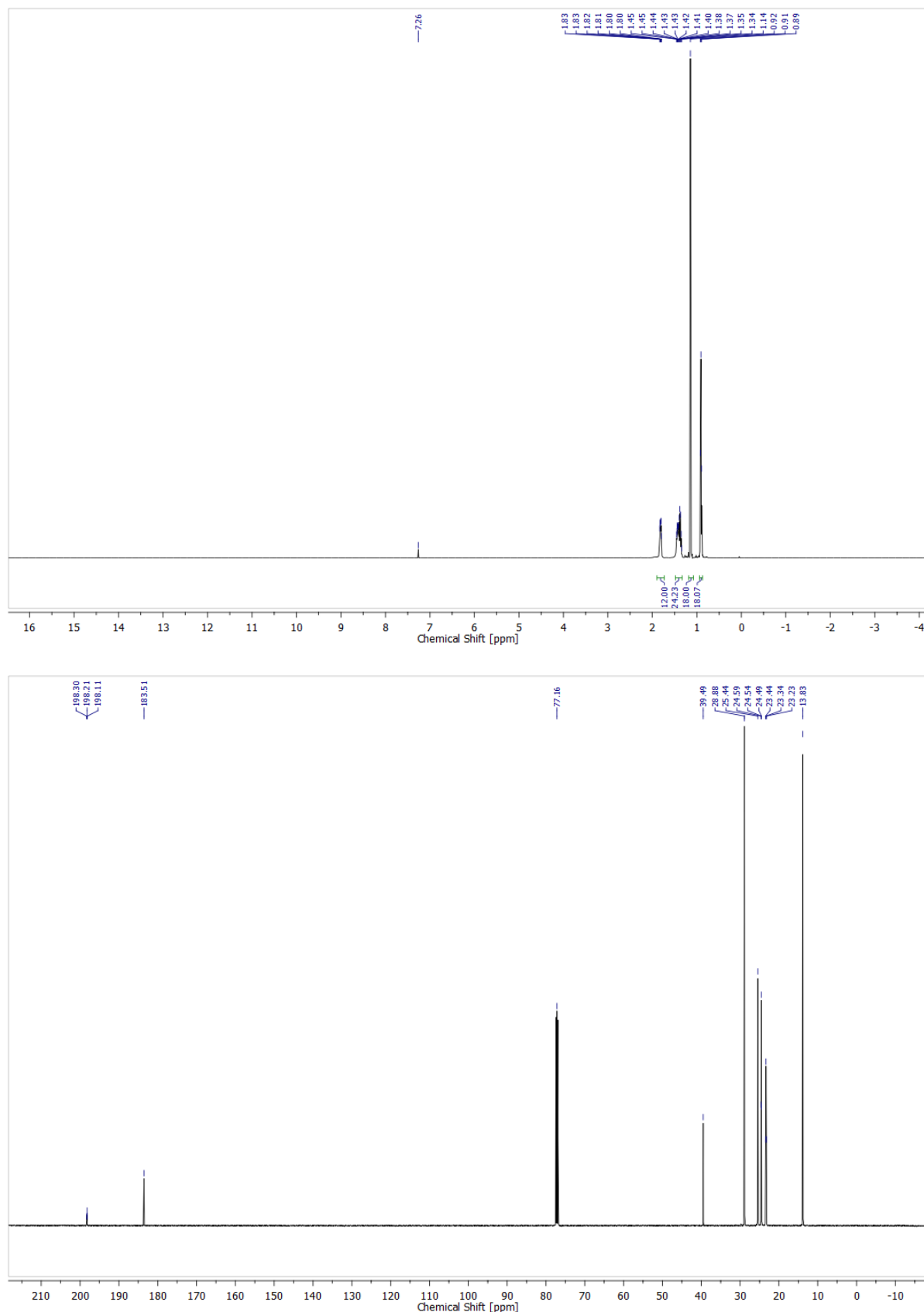
Ru(CO)₂(PⁿBu₃)₂(O₂CCH₂CH₃)₂ (4b**)**



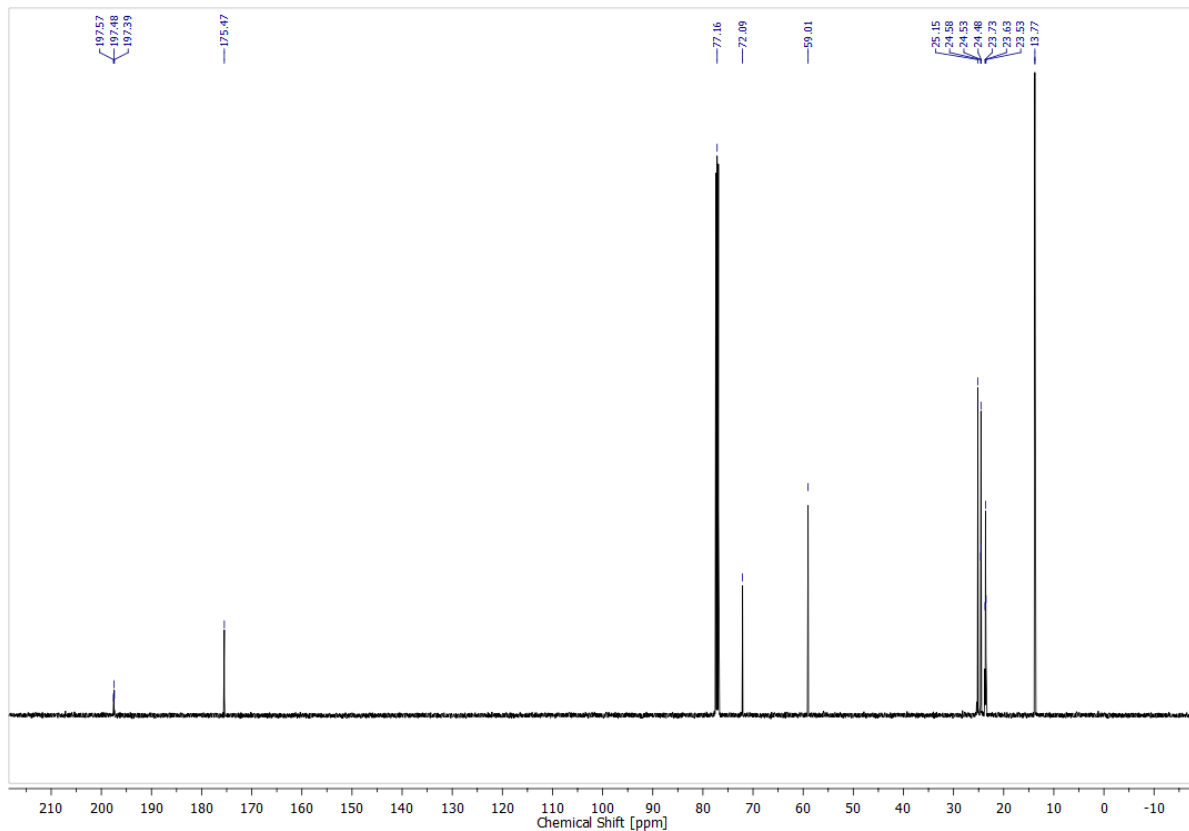
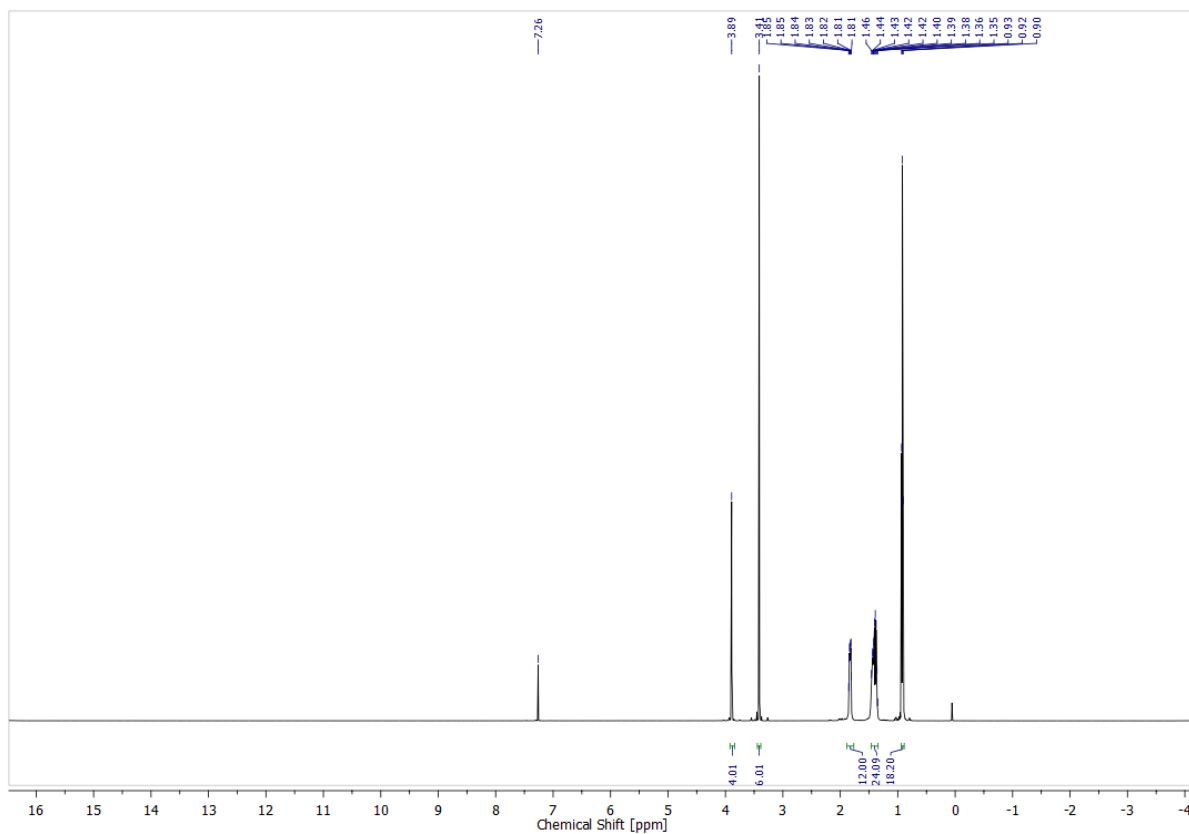
Ru(CO)₂(PⁿBu₃)₂(O₂CCH(CH₃)₂)₂ (4c**)**



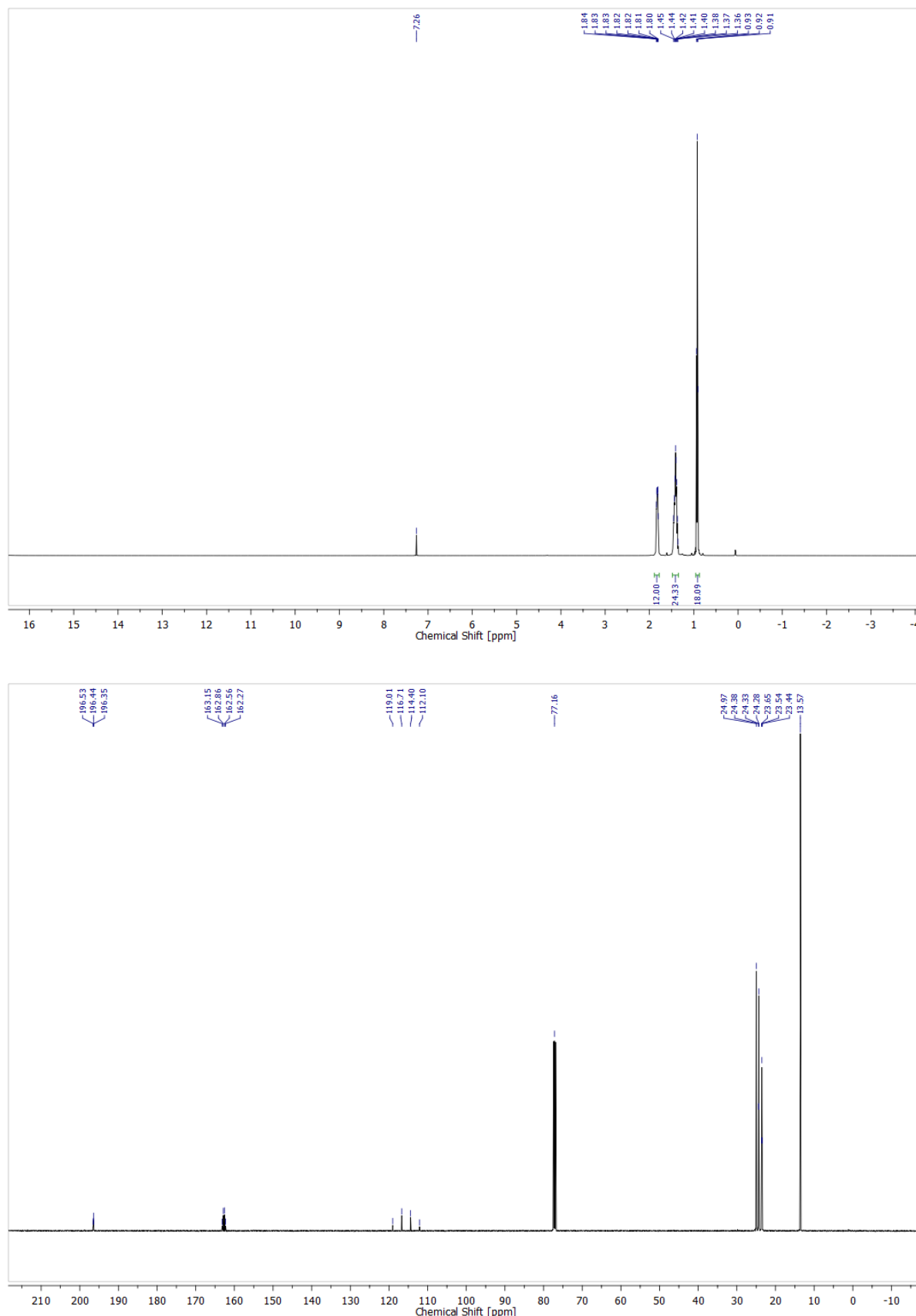
Ru(CO)₂(PⁿBu₃)₂(O₂CC(CH₃)₃)₂ (4d**)**



Ru(CO)₂(PⁿBu₃)₂(O₂CCH₂OCH₃)₂ (4e**)**



Ru(CO)₂(PⁿBu₃)₂(O₂CCF₃)₂ (4f**)**



Ru(CO)₂(PⁿBu₃)₂(O₂CCF₂CF₃)₂ (4g**)**

